Three-dimensional finite element analysis of a novel interzygapophyseal fusion device for lower cervical spine

QI WANG[1, 2], HONG YUAN[1], MINGMING GUO[1], LINGZHI MENG[1],
ZUOYAO LONG[1], YU LONG[1], HUIFENG YANG[1, 2]*

[1] Department of Orthopedics, General Hospital of Northern Theater Command, Shenyang, Liaoning Province, China.
[2] China Medical University, Shenyang, Liaoning Province, China.

Purpose: A three-dimensional finite element model of the lower cervical spine was established to evaluate the biomechanical stability and stress distribution of the new lower cervical interzygapophyseal fusion device (IZFD) developed by ourselves under different construct. The aim of this study was to provide theoretical basis for further clinical application. *Methods*: A normal fresh cadaveric specimen (male, 35 years old) was used to establish an intact three-dimensional finite element model of C3–C6. On this basis, the comparative finite element models of the lateral mass screw rod (LMSR) system and LMSR+IZFD were established. Only C4–C5 is fixed in the lateral mass. The range of motion (ROM) and stress distribution in the flexion,extension, lateral bending and rotation of the C4–C5 segment under the three constructs were analyzed. *Results*: The ROM and stress distribution of the three-dimensional finite element model under load construct were within a reasonable range, which proved the validity and reliability of the model. The ROM and stress distribution of C4–C5 segment was significantly decreased in both LMSR and LMSR+IZFD constructs than those in the intact construct. The ROM and stress distribution were even smaller in LMSR+IZFD construct than in LMSR construct. *Conclusions*: The IZFD combined with LMSR system can provide satisfactory stability for the lower cervical spine, and the IZFD can further improve the fixation effect of the LMSR system.

Key words: three-dimensional finite-element analysis, interzygapophyseal fusion device, lower cervical spine, facet joint

1. Introduction

Posterior cervical lateral mass screw rod (LMSR) system and bone graft fusion is a commonly surgical approach. However, there are disadvantages such as more bleeding, bone graft displacement and low fusion rate during posterolateral bone grafting [6]. The facet joint is an important structure for cervical spine stability [1], [2], [8], [10], [14], [15], [17]. If the fusion between the facet joints can be achieved, the posterolateral bone graft can be completely replaced, thereby avoiding the occurrence of the above adverse events. Facet fusion cage is an ideal method to promote vertebral fusion, but there are few reports on the application of lower cervical facet cage. Based on this, we designed a screw-shaped lower cervical interzygapophyseal fusion device (IZFD, ZL 2015 2 0038584.9) made of porous titanium, which can be quickly 3D printed, providing a new method for posterior cervical fusion. However, its biomechanical properties have not been studied yet.

The biomechanical analysis is a good method to evaluate the operative trauma and reconstruction effects of spine surgery [3]. Finite element analysis (FEA) is the theoretical biomechanical research to perform numerical stress analysis by the computational biomechanical testing technology [19]. With the development of computer and software technology, the current three-dimensional nonlinear model can not

---

only simulate the vertebral body and intervertebral disc realistically, but also imitate the surrounding structures directly or indirectly [5], [7], [12]. Thus, as one of the biomechanical research methods, FEA can be used in the biomechanical analysis for various tissues of the cervical spine, along with spinal internal fixation instruments. Therefore, in this study, a three-dimensional finite element model of the lower cervical spine was established to study its theoretical biomechanics.

2. Materials and methods

The design of a novel interzygapophyseal fusion device (IZFD) for lower cervical spine

This study had been reviewed and approved by the ethics committee of General Hospital of Northern Theater Command (Number: k2015-39). We designed a novel IZFD for lower cervical spine, made of porous titanium alloy. The screw-shaped instrument is divided into two parts. The thread part is 9 mm in total and the tail part is 3mm. The porous structure with porosity of 0.5 is used and the grid unit is dodecahedron. In order to ensure the strength of the hexagonal hole, solid printing is used. According to the design size, the device was printed by Arcam EBM Q10 Metal 3D printer. As the 3D printing accuracy can not meet the requirements of the hexagon, we first drill the screw tail to a depth of 2 mm to 2.3 mm after printing, and then use the hexagon stamping tool to punch.

Sample collection

One male (35 years old) fresh frozen human cadaveric cervical spinespecimen (C3–C6) was used for this study. Radiographic screening was performed to exclude specimens with cervical fractures, metastatic tumors, osteopetrosis or obvious osteoporosis that could affect the biomechanics of the spine.

The establishment of three-dimensional finite element model

The Mimics software was used to import and process the DICOM (Digital Imaging and Communications in Medicine) format computed tomography (CT). Boolean operations were utilized to obtain models including small joints around the bone, intervertebral disc, and the like. Based on the 3D model data from Geomagics, the volumetric three-dimensional reconstruction was constructed and Pro/E5.0 was used to assemble the model. The vertebral model includes C3–C6 and intervertebral discs, facet joints, lateral

block screw and inter-articular joint fusion cage. In addition, the vertebrae was also distinguished between cortical bone and cancellous bone.

The porous structure was modeled by magics19.0. Through the replicatiom and expansion of the porous single crystal cell, the surface of the original implant nail was wrapped to form a porous structure with controlled porosity (Figs. 1A, B). The porosity is calculated as follows: V1–V2/V1; where V1 is the original implanted nail volume without voids and V2 is the porous structure implanted nail volume.
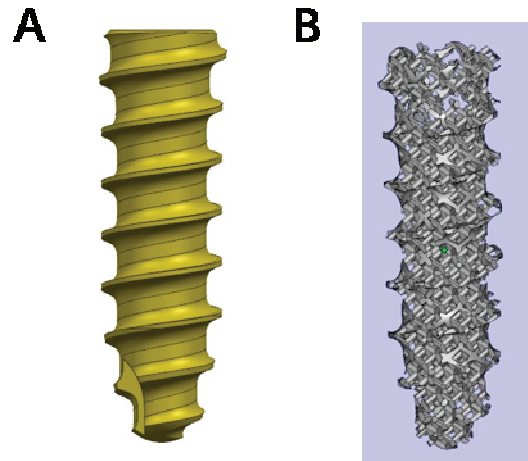

Fig. 1. The novel designed IZFD. The schematic diagram (A) Model (B) of IZFD.
IZFD: Interzygapophyseal fusion device ()

The inferior surface of the C6 was fixed, distribution load was applied on the superior endplate of C3. The model load parameters were set based on the load parameters in the reference: skull load 73.6 N, torque load 1 N·m, C6 bottom fixed constraint. Five pairs of contact pairs from C3 to C6 were established in this model and the contact pair setting was shown in Table 1. Under load constructss, calculations were performed under four operating conditions (anterior flexion, posterior extension, lateral bending, and rotation). The main parameters observed were range of motion (ROM) and stress diagrams. The former can represent the segmental angular displacement and the latter can show the stress on the lateral mass screw fixation and IZFD [9], [16].

Table 1. Contact pair settings

No.		Contact pair settings
1	Vertebra VS Intervertebral disc	Bond
2	Vertebra VS Facet joint	Bond
3	Facet joint VS Facet joint	Contact
4	Reference point VS Vertebra	Coupling
5	Implant VS Bone or Facet joint	Bond

On this basis, the comparative finite element models of the lateral mass screw rod (LMSR) system and LMSR+IZFD were established. Only C4–C5 is fixed in the lateral mass. The range of motion (ROM) in the flexion, extension, lateral bending and rotation under the three constructs were analyzed.

3. Results

Parameters of the IZFD and the elements contained in the Model

The novel IZFD was designed based on our clicnial experience. The outer diameter of the fusion device thread was 3.5 mm, with the inner diameter of 2.6 mm, the total length of 5–10 mm and the thread width of 0.14 mm. The inner hexagon was SW 2.0 mm (edge to edge distance), with the depth of 2 mm and the hole depth of 2.3 mm. The head of the tap (3.5 mm in diameter and 15 mm in length) was made of 17-4PH medical stainless steel and is tapered to screw it into the facet joint space. The thread width was 0.14 mm and the inner diameter was 2.4 mm, which was slightly smaller than the inner diameter of the screw to increase the holding force. The screw is divided into two parts: the thread part is 9 mm in total and the other is porous structure with porosity of 0.5.

The construct included the following aspects: Intact (Fig. 2A), single bilateral lateral mass screw rod (LMSR) system (Fig. 2B) and bilateral LMSR system combined with IZFD (Fig. 2C). The ligaments include the anterior longitudinal ligament, the posterior longitudinal ligament, the ligamentum flavum, the intertransverse ligament and the interspinous ligament. The types of mesh units were shown in Tables 2 and 3, where the

number of three-dimensional tetrahedral meshes was 428 475 and the one-dimensional link 180 cells are 285. The total number of units was 428 760 and the total number of nodes was 309 583.

Table 2. Grid type and unit amount

Name	Unit type
Vertebral body	Solid186
Vertebral cancellous bone	Solid186
Pedicle of vertebral arch	Solid186
Facet joint	Solid186
End plate	Solid186
Nucleus pulposus	Solid186
Annulus fibrosus	Solid186
Anterior longitudinal ligament	Link180
Posterior longitudinal ligament	Link180
Ligamentum flava	Link180
Capsular ligament	Link180
Intertransverse ligament	Link180
Interspinal ligament	Link180

Table 3. Unit and node amount in different construct

Construct	Unit amount	Node amount
Intact	428,760	309,583
LMSR	426,336	353,249
LMSR+IZFD	439,981	360,645

Verification of the effectiveness of the models

Under load construct, the angular displacements of the C3–C6 segments in the three-dimensional finite element model were calculated under four operating conditions (cervical spine anterior flexion, posterior extension, lateral bendingand rotation). The results showed that the angular displacement of the C3–C4 segment under the condition of cervical spine anterior
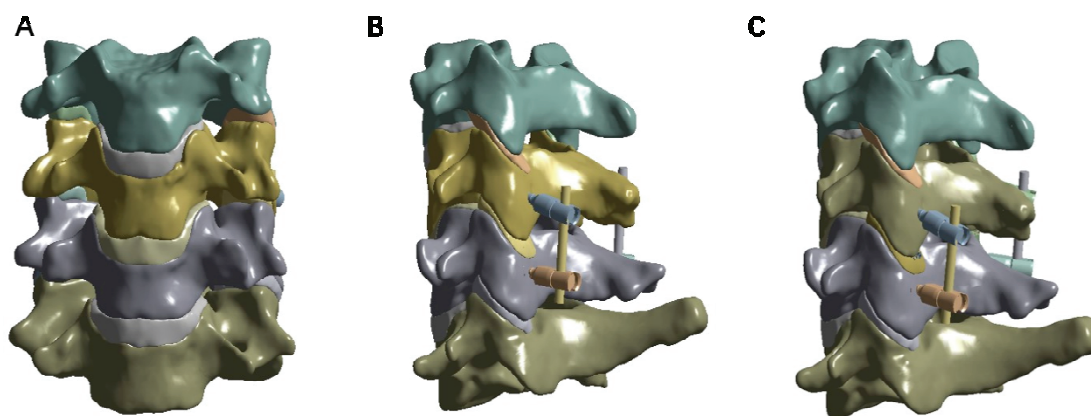

Fig. 2. Three dimensional model in the experiment: (A) intact model, (B) bilateral LMSR fixation,
(C) bilateral LMSR fixation combined with IZFD.
LMSR – Lateral mass screw rod, IZFD – Interzygapophyseal fusion device

flexion was 5.71, the angular displacement of the C4–C5 segment was 4.87, the angular displacement of the C5–C6 segment was 4.30. The angular displacement of the C3–C4 segment under the condition of posterior extension was 4.00, the angular displacement of the C4–C5 segment was 4.12, the angular displacement of the C5–C6 segment was 3.67. The angular displacement of the C3–C4 segment under the condition of lateral bending was 3.95, the angular displacement of the C4–C5 segment was 3.48, the angular displacement of the C5–C6 segment was 2.87. The angular displacement of the C3–C4 segment under the condition of rotation was 2.87, the angular displacement of the C4–C5 segment was 2.91, the angular displacement of the C5–C6 segment was 2.65. The activity of each segment was basically within the range of reasonable

results (Table 4) and was consistent with the results of Panjabi's [13]. Thus, we concluded that this 3D finite model was effective under certain conditions and its validity was proved.

According to the load construct analysis, the MISES stress of intervertebral disc(IVD) is associated with the operating conditions. The MISES stress was concentrated on the front of IVD under flexion condition, while it was fastened on the back of IVD in case of extension. On the condition of bending, we found the stress concentration in the two sides of IVD. When the rotation occurred, the stress distribution was relatively even. Similar to previous study, the MISES stress of IVD was basically in the range of 0.7 MPa–1.9 MPa. Thus, the disc modeling method is relatively realistic and it is closer to the true tissue stress distribution.
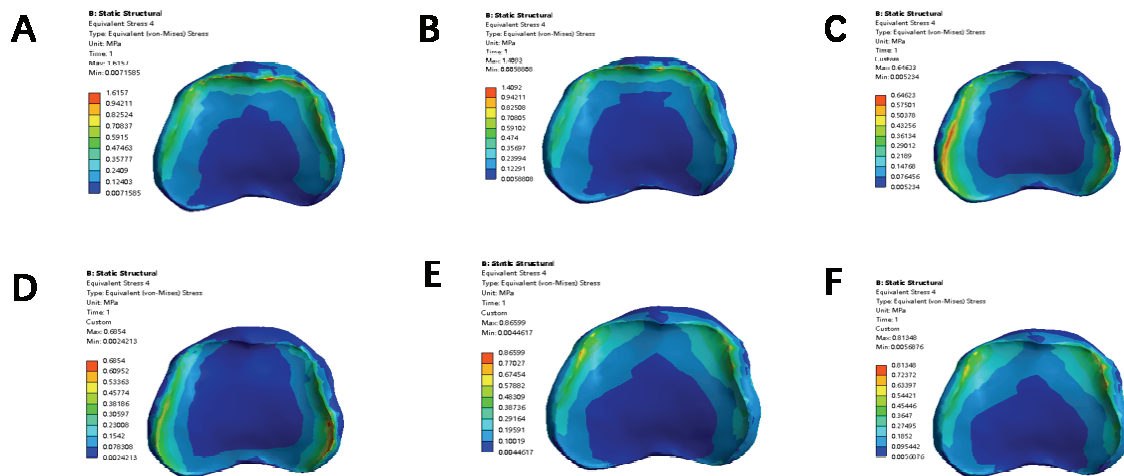

Fig. 3. The Stress distribution of C4-5IVD in intact construct under different conditions:
(A) flexion, (B) extension, (C) left bending, (D) right bending, (E) left rotation, (F) right rotation.
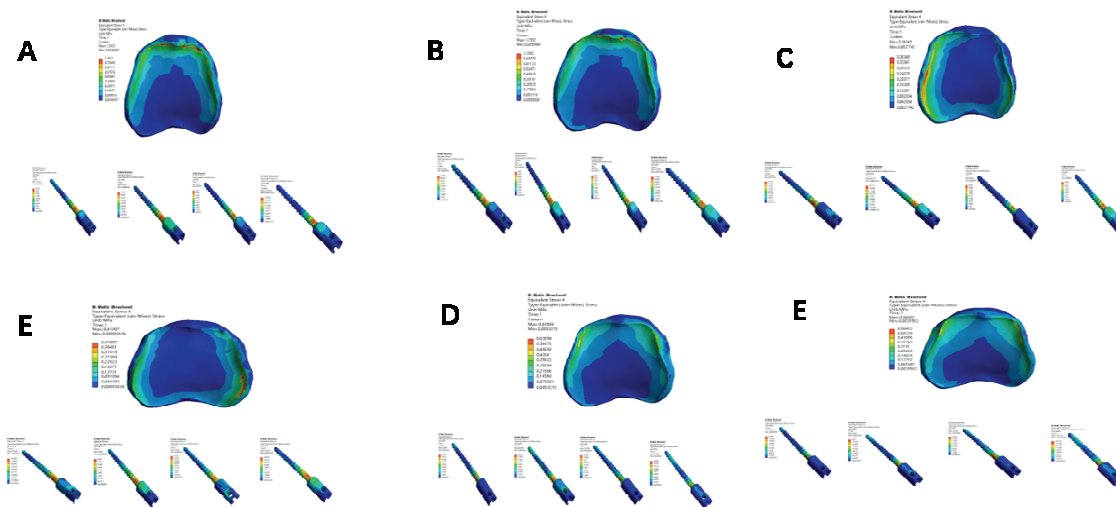ROM – Range of motion, IVD – Intervertebral disc

Fig. 4. Stress distribution of C4-5 IVDin LMSR construct:
(A) flexion, (B) extension, (C) left bending, (D) right bending, (E) left rotation, (F) right rotation.
IVD – Intervertebral disc, LMSR – Lateral mass screw rod

The ROM of C4–C5 segment

Under flexion condition, the ROM of intact construct was 4.81, while the ROM in the LMSR and LMSR + IZFD construct was 1.52 and 1.01 respectively. Other conditions had similar tendency, and the ROM of different construct were as follows: under extension condition, 4.17 for intact construct, 2.25 for LMSR construct, 1.44 for LMSR + IZFD construct; under left bending condition, 3.49 for intact construct, 2.32 for LMSR construct, 1.63 for LMSR + IZFD construct; under right bending condition, 3.34 for intact construct, 2.23 for LMSR construct, 1.51 for LMSR + IZFD construct; under left rotation condition, 2.86 for intact construct, 1.85 for LMSR construct, 0.91 for LMSR + IZFD construct; under right rotation condition, 2.75 for intact construct, 1.77 for LMSR construct, 0.85 for LMSR + IZFD construct (Table 5). Compared with intact construct , the ROM was decreased with the fixation of LMSR or LMSR + IZFD construct, due to the roles of IZFD, the ROM of LMSR + IZFD construct was smaller than that in LMSR construct.

Stress distribution of the C4–C5 IVD
under the intact, LMSR and
LMSR + IZFD construct in finite element model

Under flexion condition, the maximum stress of intact construct was 1.6157 MPa (Fig. 3A), while the maximum stress concentration in the LMSR and LMSR + IZFD construct was 1.3822 MPa (Fig. 4A) and 1.0936 MPa (Fig. 5A), respectively. Other con-

ditions had similar tendency, and the maximum stress of different conditions was as follows: under extension condition, 1.4092 MPa (Fig. 3B) for intact construct, 1.1592 MPa (Fig. 4B) for LMSR construct, 1.0936 MPa (Fig. 5B) for LMSR+IZFD construct; under left bending condition, 0.64623 MPa (Fig. 3C) for intact construct, 0.36349 MPa (Fig. 4C) for LMSR construct, 0.12109 MPa (Fig. 5C) for LMSR + IZFD construct; under right bending condition, 0.6854 MPa (Fig. 3D) for intact construct, 0.41007 MPa (Fig. 4D) for LMSR construct, 0.12109 MPa (Fig. 5D) for LMSR + IZFD construct (; under left rotation condition, 0.86599 MPa (Fig. 3E) for intact construct, 0.63694 MPa (Fig. 4E) for LMSR construct, 0.5917 MPa (Fig. 5E) for LMSR + IZFD construct; under right rotation condition, 0.81348 MPa (Fig. 3F) for intact construct, 0.56482 MPa (Fig. 4F) for LMSR construct, 0.5917 MPa (Fig. 5F) for LMSR + IZFD construct. Compared to intact construct, the MISES stress of IVD was decreased with the fixation of LMSR or LMSR + IZFD, due to the role of IZFD, the maximum stress of LMSR + IZFD construct was smaller than that in LMSR construct.

4. Discussion

The facet joint plays an important role in maintaining the stability of the cervical spine. Resection of the facet joint has different effects on the biomechanics of the cervical spine. Zdeblick [20] analysed the
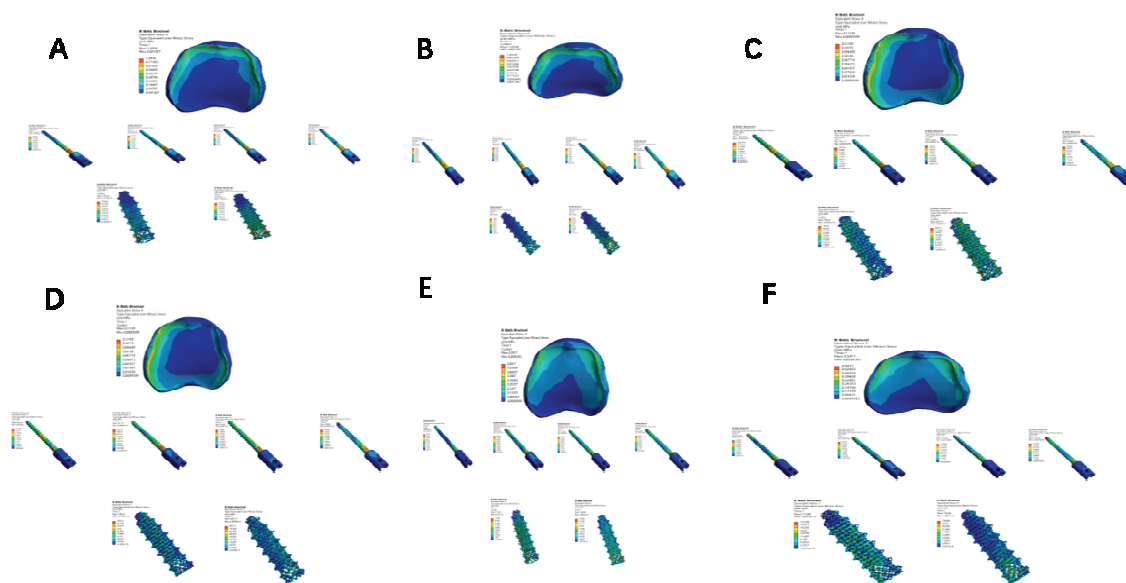

Fig. 5. Stress distributionof C4–C5 IVD in LMSR and IZFD construct:
(A) flexion, (B) extension, (C) left bending, (D) right bending, (E) left rotation, (F) right rotation.
IVD – Intervertebral disc, LMSR – Lateral mass screw rod, IZFD – Interzygapophyseal fusion device

biomechanical characteristics of 12 human cervical spine specimens after intervertebral foramen resection. After 50% of the facet joints were removed, the torsional stiffness decreased significantly, and the posterior strain increased by 2.5%, which would lead to cervical segmental hyperactivity. When 75% or 100% of the facet joints were removed, the posterior strain increased by 25%. In a shear test of cervical motor segments, including two vertebral bodies and surrounding structures, Richard found that when the facet joint was removed by more than 50%, its shear strength was significantly reduced [14].

Therefore, the fusion of facet joint is very important in posterior cervical fusion. Facet fusion cage is a relatively new way to promote vertebral fusion. Voronov [18] reported in 2016 that the posterior cervical square interbody fusion cage could significantly improve the stability compared with single segment and multi segment anterior cervical discectomy and fusion (ACDF). Therefore, the posterior cervical interbody fusion cage may be a potential and minimally destructive supplementary fixation method to improve the fusion rate of ACDF. McCormack [11] had developed an instrument for the removal of articular cartilage in the posterior cervical facet without laminectomy, which minimized soft tissue injury. Goel [4] reported facet joint spacers were used to treat cervical spinal stenosis. The purpose of our design is to achieve posterior cervical interbody fusion and minimize soft tissue injury. Compared with previous reports, the advantages are: 1) the screw-shaped fusion cage is convenient to screw in and out; 2) There is a matching screw-shaped articular cartilage removal device; 3) The fusion cage is made of porous titanium material with good biocompatibility with human body; 4) It has a microporous structure similar to human cancellous bone, which is conducive to bone growth, so as to promote facet joint fusion; 5) It simplifies the surgical procedure, reduces the interference to the spinal cord, and avoids the disadvantages of excessive bleeding, displacement of the bone graft, non-fusion, and complications related to the harvesting of the autologous bone during the posterolateral bone grafting.

In this study, the ROM of each segment of the intact cervical spine was compared with the biomechanical test results of the specimens reported in the literature. Within reasonable results, the effectiveness of this model is demonstrated. This model could accurately simulate the system structure, material and mechanical characteristics of the LMSR system and the interzygapophyseal fusion device (IZFD) after implantation. The established finite element model was convenient, reasonable and realistic. It can be used for analysis and reconstruction of the lower cervical spine and implantation of the lower cervical articular facet.

After implanting the LMSR system, the ROM and stress distribution of the C4–C5 segment under the conditions of flexion, extension, left and right lateral bending, and left and right rotation was significantly reduced compared to the intact model, while the lower cervical IZFD was implanted. The ROM and stress distribution was further reduced. It showed that the stability of the lower cervical spine was further improved after the implantation of the lower cervical IZFD. As we all known, the results of *in vitro* tests in this study are not comparable to those of *in vivo* tests. Thus, in order to further validate the applicability of the novel designed IZFD, What we are going to do is to explore its biomechanical characteristics and long-term facet joint fusion in vivo model.

Abbreviations

IZFD	–	interzygapophyseal fusion device,
FE	–	flexion extension,
IVD	–	intervertebral disc,
ROM	–	range of motion,
CT	–	computed tomography,
F	–	flexion,
E	–	extention,
LB	–	left bending,
RB	–	right bending,
LR	–	left rotation,
RR	–	right rotation.

Ethical approval and consent to participate

Availability of data and materials

The datasets are available from the corresponding authors on reasonable request.

Competing interests

The authors declare that they have no conflict of interest.

Funding

Authors' contribution

QI WANG and HONG YUAN contributed equally to this work.

References

[1] CHENG N.S., LAU P.Y., SUN L.K., WONG N.M., *Fusion rate of anterior cervical plating after corpectomy*, J. Orthop. Surg. (Hong Kong), 2005, 13 (3), 223–227, DOI: 10.1177/ 230949900501300302.

[2] CUSICK J.F., YOGANANDAN N., PINTAR F., MYKLEBUST J., HUSSAIN H., *Biomechanics of cervical spine facetectomy and fixation techniques*, Spine (Phila, Pa, 1976), 1988, 13 (7), 808–812.

[3] GANDHI A.A., KODE S., DEVRIES N.A., GROSLAND N.M., SMUCKER J.D., FREDERICKS D.C., *Biomechanical Analysis of Cervical Disc Replacement and Fusion Using Single Level, Two Level, and Hybrid Constructs*, Spine, 2015, 40, 1578–1585, DOI: 10.1097/brs.0000000000001044.

[4] GOEL A., SHAH A., *Facetal distraction as treatment for single- and multilevel cervical spondylotic radiculopathy and myelopathy: a preliminary report*, J. Neurosurg. Spine, 2011, 14 (6), 689–696, DOI: 10.3171/2011.2.SPINE10601.

[5] HEDENSTIERNA S., HALLDIN P., *How does a three-dimensional continuum muscle model affect the kinematics and muscle strains of a finite element neck model compared to a discrete muscle model in rear-end, frontal, and lateral impacts*, Spine, 2008, 33, E236-245, DOI: 10.1097/ BRS.0b013e31816b8812.

[6] KANEMATSU R., HANAKITA J., TAKAHASHI T., MINAMI M., INOUE T., HONDA F., *Risk Factor Analysis of Facet Fusion Following Cervical Lateral Mass Screw Fixation with a Minimum 1-Year Follow-up: Assessment of Maximal Insertional Screw Torque and Incidence of Loosening*, Neurol. Med. Chir. (Tokyo), 2021, 61 (1), 40–46, DOI: 10.2176/ nmc.oa.2020-0206.

[7] KARADOGAN E., WILLIAMS R.L., *Three-dimensional static modeling of the lumbar spine*, Journal of Biomechanical Engineering, 2012, 134, 084504, DOI: 10.1115/ 1.4007172.

[8] KATO Y., KANEKO K., KATAOKA H., KOJIMA T., IMAJYO Y., TAGUCHI T., *Cervical hemilaminoplasty: technical note*, Journal of Spinal Disorders and Techniques, 2007, 20, 296–301, DOI: 10.1097/01.bsd.0000211287.98895.a3.

[9] KHUYAGBAATAR B., KIM K., PARK W.M., KIM Y.H., *Influence of sagittal and axial types of ossification of posterior longi-tudinal ligament on mechanical stress in cervical spinal cord: A finite element analysis*, Clin. Biomech. (Bristol, Avon), 2015, 30, 1133–1139.

[10] KUROKAWA R., KIM P., *Cervical Laminoplasty: The History and the Future*, Neurologia Medico-Chirurgica, 2015, 55, 529–539, DOI: 10.2176/nmc.ra.2014-0387.

[11] MCCORMACK B.M., DHAWAN R., *Novel instrumentation and technique for tissue sparing posterior cervical fusion*, J. Clin. Neurosci., 2016, 34, 299–302, DOI: 10.1016/ j.jocn.2016.08.008.

[12] NG H.W., TEO E.C., *Nonlinear finite-element analysis of the lower cervical spine (C4–C6) under axial loading*, Journal of Spinal Disorders, 2001, 14, 201–210, DOI: 10.1097/00002517-200106000-00003.

[13] PANJABI M.M., WHITE A.A. 3rd, JOHNSON R.M., *Cervical spine mechanics as a function of transection of components*, J. Biomech., 1975, 8 (5), 327–336.

[14] RAYNOR R.B., PUGH J., SHAPIRO I., *Cervical facetectomy and its effect on spine strength*, J. Neurosurg., 1985, 63 (2), 278–282.

[15] TANAKA N., FUJIMOTO Y., AN H.S., IKUTA Y., YASUDA M., *The anatomic relation among the nerve roots, intervertebral foramina, and intervertebral discs of the cervical spine*, Spine, 2000, 25, 286–291, DOI: 10.1097/00007632-200002010-00005.

[16] TASO M., FRADET L., CALLOT V., ARNOUX P.J., *Anteroposterior compression of the spinal cord leading to cervical myelopathy: a finite element analysis*, Comput. Methods Biomech. Biomed. Engin., 2015, 18 (Suppl 1), 2070–2071.

[17] VOO L.M., KUMARESAN S., YOGANANDAN N., PINTAR F.A., CUSICK J.F., *Finite element analysis of cervical facetectomy*, Spine, 1997, 22 (9), 964–969.

[18] VORONOV L.I., SIEMIONOW K.B., HAVEY R.M., CARANDANG G., PHILLIPS F.M., PATWARDHAN A.G., *Bilateral posterior cervical cages provide biomechanical stability: assessment of stand-alone and supplemental fixation for anterior cervical discectomy and fusion*, Med. Devices (Auckl.), 2016, 9, 223–230, DOI: 10.2147/MDER.S109588, eCollection 2016.

[19] WU T.K., MENG Y., LIU H., WANG B.Y., HONG Y., RONG X., DING C., CHEN H., *Biomechanical effects on the intermediate segment of noncontiguous hybrid surgery with cervical disc arthroplasty and anterior cervical discectomy and fusion: a finite element analysis*, The Spine Journal: official journal of the North American Spine Society, 2019, 19, 1254–1263, DOI: 10.1016/j.spinee. 2019.02.004.

[20] ZDEBLICK T.A., ZOU D., WARDEN K.E., MCCABE R., KUNZ D., VANDERBY R., *Cervical stability after foraminotomy. A biomechanical in vitro analysis*, J. Bone Joint Surg. Am., 1992, 74 (1), 22–27.